The Investigation of an Efficient and Effective Proactive Pipeline Integrity System

Masoud Forsat
m.forsat@qu.edu.qa
Department of Mechanical and Industrial Engineering, Qatar University, Doha, Qatar

Abdelmagid S. Hamouda
hamouda@qu.edu.qa
Department of Mechanical and Industrial Engineering, Qatar University, Doha, Qatar

ABSTRACT

In this paper, we propose the investigation of an efficient and effective proactive pipeline integrity system that uses multi-sensors for monitoring and inspection of the pipeline. Although the focus is on the pipeline, the methodologies will also be applicable for other systems including other energy infrastructure elements. The investigation focuses on the integration of multi-sources of data as well as multi-types of data for the same location (section) of the pipeline. The data include imaging, acoustic signals, electromagnetic flux system, and others. Moreover, the data could be obtained using continuous monitoring of the pipeline sections or through time intervals. In both cases, the data may also include censored observations. We develop several approaches to filter the data for noise and identify outliers, integrate the data streams into one degradation path and determine the optimum time to maintain or replace the pipeline sections being monitored. It will utilize extensive mathematical modeling for condition-based maintenance and repair, which will be developed by the investigators of this proposal. Following the suggestions of one of the reviewers of the last year's submission, we plan to validate and modify the model using standard or artificially developed defects such as corrosion, cracks, stress cracking, etc. to understand the output of the proposed methodology and validate the models accordingly.

Keywords: Pipeline; Infrastructure; Integrity system; Crack detection

1 INTRODUCTION

Regarding that the use of pipelines in the industries has been widened, and any leakage of their valuable or hazardous liquids could result in serious environmental problems, the attention to the faults and damages types and reason are compulsory for users and authorities. Structural damages caused by fault action are attracting much attention from engineers and researchers in recent years. The reasons for the pipelines damage are corrosion, cracks, vibration (Forsat, 2019), loads (Mirjavadi, Forsat et al., 2019) and etc. Also, a wide variety of damage detection and health monitoring of them have been used which including fiber optical sensors and piezoceramic transducer (Zeng, Dong et al. 2019). A lot of investigation on the pipeline damages detection and dynamic responses of the metals has been done (Mirjavadi, Forsat et al., 2019) and the results can be categorized to two overall sections, Visual Inspection and Computerized Inspection. Visual inspection mostly done by the some methods like NDT or ultrasonic (Lowe, Alleyne et al., 1998; Chang, Zi et al., 2017) and another method is computer

vision that has developed these days, is by the use of computer software and different kinds of analyzing (Jin, Zhang et al., 2014; Chen, Zhou et al., 2019; Mirjavadi, Forsat et al., 2019). The computerized inspection method is an economical and more appropriate replacement to the traditional and dangerous techniques of inspection of a pipeline, especially if a pipeline carrying dangerous liquids, flammable or be too small for human entry (Bahadori, 2017; Hawari, Alamin et al., 2018). In some industries that they have deep-water pipeline, the use of computer vision method is undeniable. The investigations on the marine deep water pipeline showed the importance of using internal damage detector machine controlling by the computers (Mao, Chu et al., 2015). The use of wireless sensors networks (WSN) for designing of the cost-effective leak detective system has been investigated. The experimental results showed the improvements of the WSN to other techniques in the context of damage detection in the monitoring water pipeline process (Ayadi, Ghorbel et al., 2019). The problem of pipe damaging is more important in gas transportation industries because any leakage in this system is hard to see by normal methods and most of them are dangerous liquids. An investigation on the acoustic wave detection system has been done in many researches (Sousa, Cruz et al., 2009; Xu, Zhang et al., 2013; Liu, Li et al., 2017; Zajam, Joshi et al., 2019). At the first stage, the phonation principle of the leakage and the characteristic of the sound source has been investigated and then the simulation of the leakage acoustic field has been done. The results showed the detection system could identify small gas leakage effectively and avoids false-alarms which caused by running conditions with a good prospect (Xu, Zhang et al., 2013). Specific routine and special operations are essential in order to maintain an efficient, reliable, and economic pipeline operation. These operations may be caused by hydrate formation, formation of inorganic deposits, transported product contamination and etc. (Stewart, 2016). The development of the many different monitoring devices and their modification and improvement over time have allowed the pipeline industry to be able to monitor all of the metal pipes and structures desired (Singh, 2017).

2 EXPERIMENTAL WORK

For the starting of the experimental works and testing of the robot and our simulation works, a circulate pipeline setup has been prepared (Fig 1). The setup consists of a water pump, 16cm thickness of pipes, three L bolts, and one water tank. The pipes were held by the hanging rods (Pipeline holder) to avoid any vibration on them and make them stable at their position. In addition, the temperature of the tanker is controlled by a thermostat for different water temperatures.

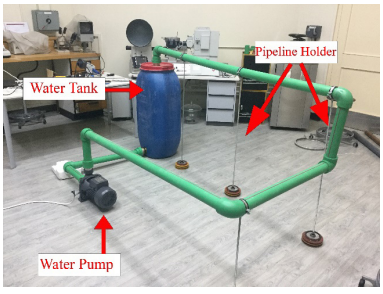

Figure 1: Pipeline setup details

The main robot will move through the pipeline while it takes data like images, recorders and etc. from whole sides of the pipe (Fig 2). After that, the collected data will exposure to several different image processing to classify in their own group. The different groups of images will be categorized by the type and shape of the damages on the pipe. As a result, the damages on the pipeline will be clear to identify and make a good decision for their maintenance.

The main components of the machine are: C arm, Gearwheel, Gear holder, and Robot holder

These parts help the image capturing robot to move through the pipeline system so they act as the mechanical part of the system that are responsible for controlling the movements.

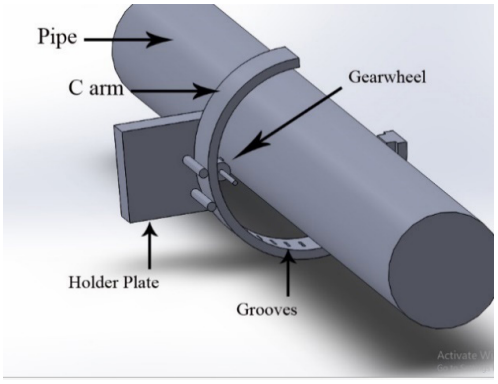

Figure 2: The components of the system

The first part of the machine is the arm that entitled C arm because of its shape that is the 3/4 a circle (Fig 3). With this arm, the camera can rotate around the pipe to capturing the images. It is consist of a cylindrical gear wheel that doing the rotating duty. In addition, it has two lockers in the ends of the circle to avoiding getting out of the ring the movement of this arm is along the pipeline system. Moreover, there are four ratchets on the gearwheel to lock with the grooves on this C arm. Also in each grooves of C arm, the light entitled SMD LED is placed for increasing the brightness and get a better quality of images (Fig 4). The C arm is constant and not rotating around the pipeline.

Another part of the device is the Gearwheel. In one side, the gearwheel is connected to C arm and on the other side is connected to the holder plate. With the rotating of this gearwheel, the holder plate will move around the pipe and the capturing robot can collect its data. The rotating clockwise and vice versa can control the direction of plate movement. The rotation speed of gearwheel is constant but the direction of movement will change automatically to cover all aspects of the pipeline. Also, there are two cylindrical shafts behind the C arm to keep the holder plate away from the probable vibration.

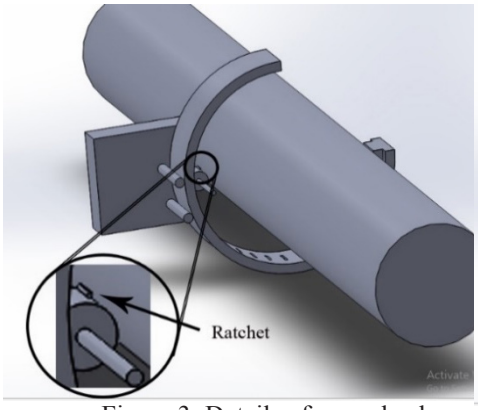

Figure 3: Details of gearwheel

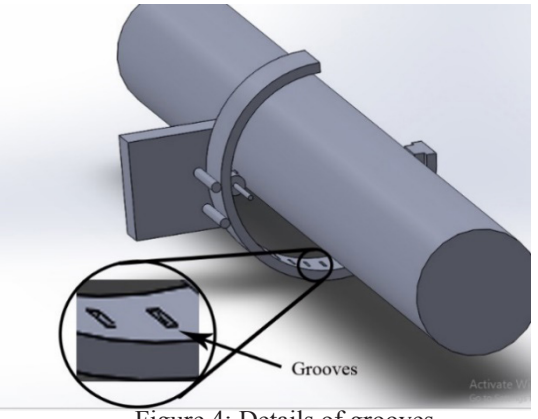

Figure 4: Details of grooves

The last part of the machine is the holder plate, which the camera will be placed on this plate. This plate has connected to the C arm by two cylindrical shafts and one gearwheel. The camera has a flexible place and it is capable to change its degree of capturing based on the situation of the plate. By this, the pipeline always will be in the vision of the camera lens. The plate movement is perpendicular to the pipeline direction.

3 FINITE ELEMENT METHOD SIMULATION

At the first stage, for simulation of the cracks and defects on the pipes and the verification process, we considered a metal material with some probable cracks and defects on it. For this purpose, we used a punched piece of the magnesium alloy that is common to use on for aerospace industries or gas and oil industries to the lightweight and high efficiency (A. NourollahiI, Farahani et al., 2013; Mirjavadi, Forsat et al., 2019). These parts of the pipe were analyzed by SEM and finite element methods. The dies and punches utilized in the setup for shear–punch test geometry for the sample in Fig.1 consists of a flat end punch of 1.38 mm diameter and a die of 1.51mm diameter (W=9 mm). Both of these were made of hardened steel (RC 58). The machine and punch compliance was minimized [11] by coupling a linear variable differential transformer (LVDT) to the moving punch. The punch is attached to a load cell having a capacity of 3000 N. An LVDT with a travel range of 3 mm measures the displacement of the punch. All shear–punch tests were performed at room temperature using a screw driven ATS machine with a constant crosshead speed of 3×10^{-3}mm/s. The cracked in in the specimen is considered as voids or hollow pathway to control the three dimensional meshing feature. The elements employed in the whole process has 8 nodes, all of which has three degree of freedom. Since the force exerted on the specimen is vertical, for applying the load we suppose that the elements which are in direct contact with the load will be subjected to the normal force on the surface. The amount of force exerted on the top plane might be considered as the average amount of the force on the last stage in the shear punch testing.

Near the crack region, which can be considered as volumetric flaw, the stress analysis shows that the region around the sideline of the crack should contain more elements with aspect ratio, while the region far from the crack can be considered as regions, which is

not necessary to contain fine elements.

Regarding the boundary conditions, it is suggested that the whole perimeter including the three-degree-of-freedom nodes around the sample of shear punch should be fixed, it means that the amount of displacement in three main axis equals to zero.

4 RESULTS

Based on the simulations on the samples it can be seen in Fig. 5 that demonstrates some macro cracks occurred on the surface of the punch area. These cracks are formed due to the stress concentration at the edge of the cross-section area of the cylinder and on its height. Moreover, the cracks propagate in 3 main direction and also created a junction of the crack with more depth. This is because of the crack paths reaching together and then stopped propagating.

It is clear from Fig. 5, all the crushes and separated pieces, have a gradient to the down side of the picture that it states there were not equal force on the surface of the specimen.it can be induced from inequality of load balancing on its surface or the height of both dies were not equal exactly.

Another problem might happen when the dies were not parallel to each other and it is led to uneven force deviation. Fig5 shows that there is a color contrast throughout the picture because of the above-mentioned reasons. It is also worth mentioning that there is no crack and crush on the top side of the picture. Furthermore, cracks could exist before the shear punch test as a defect of the specimen and during the test started propagating.

Also, it can be considered, presence of intermetallic compounds caused to initiate the crack because of their hardness (Fig. 6). It is obvious when some crack paths combine; they reinforce each other and then propagate with a higher rate than before.

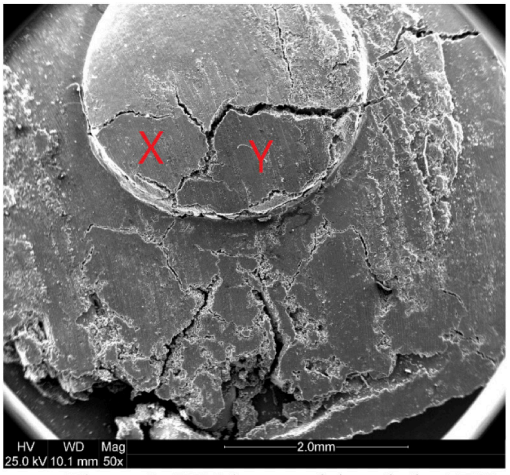

Figure 5: SEM image of the whole AZ81 shear punch surface

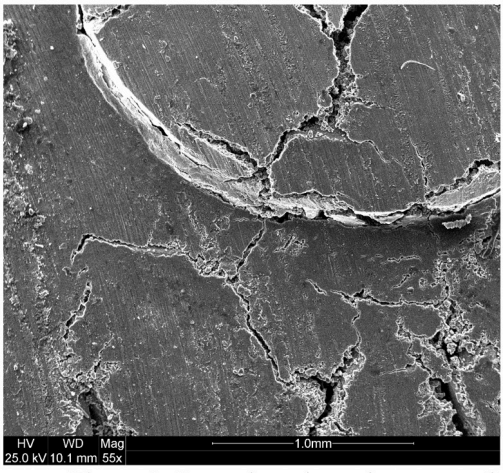

Figure 6: Created cracks at the corner of the punch effected zone (AZ81)

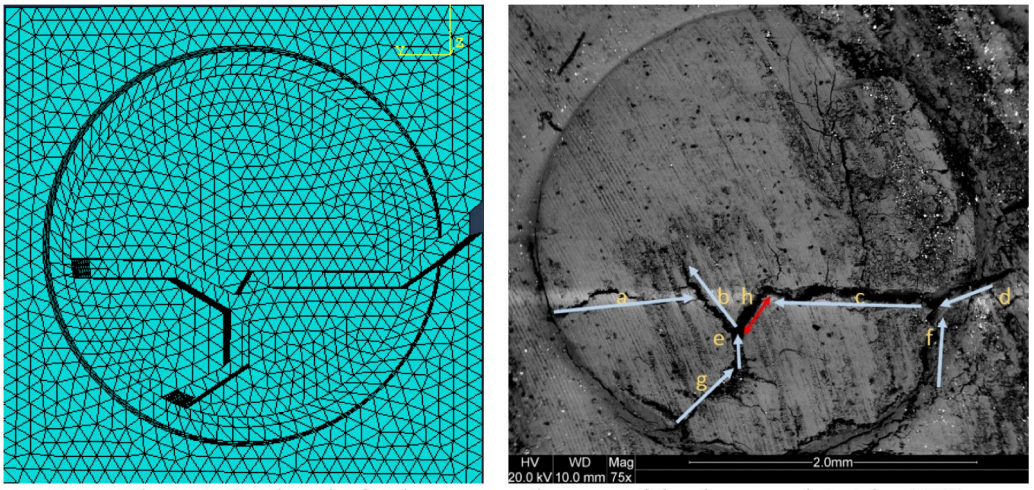

Figure 7: Crack paths for the cross-section area of the shear punch test for AZ81

Fig. 7 shows that the entire crack initiated from the zones with more stress intensity factor. As the result of this function a, d, f and also g (‘g’ itself is a combination of 2 other macro cracks). By considering Fig. 3 can understand that the width of c vector is much more than d and f vectors which induced from joining former vectors.it seems that h vector is created from 2 vectors (e and c) which cause to make a line of joining instead of junction mode. From the viewpoint of color contrast at h vector, it comes that a fully brittle zone (h) bring into being and there is no specific point of joining. Another issue is that the most width and depth occurred in this part because of associating 2 other vectors with high energy.

It must be noticed that ‘a’ vector ended with a very low width because of the crack path ended with another crack that leads to separation of two different areas. Another issue is the crushing behavior on the top of the shear punch sample to the right side and it is due to the material properties that are not dispersed throughout the sample and maybe because of accumulation of brittle secondary phases on the sample.

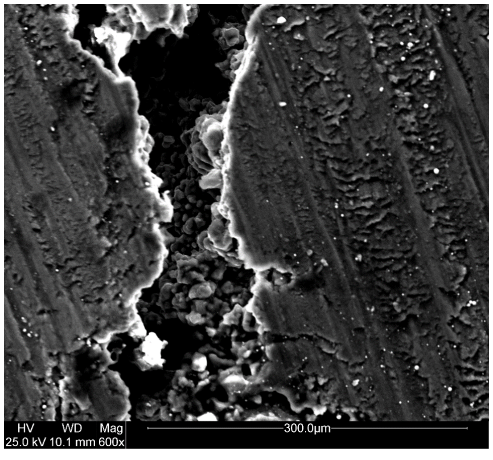

Figure 8: Macrostructure of the ‘e’ crack path in AZ81

It is obvious from Fig. 8 that a shear crack occurred in this part because of the depth of the macrocrack is not completely dark this time. Another probability is that this shear crack shape made as a result of pieces slope to the down side of the picture(X and Y area in Fig 1) in the fracture area.

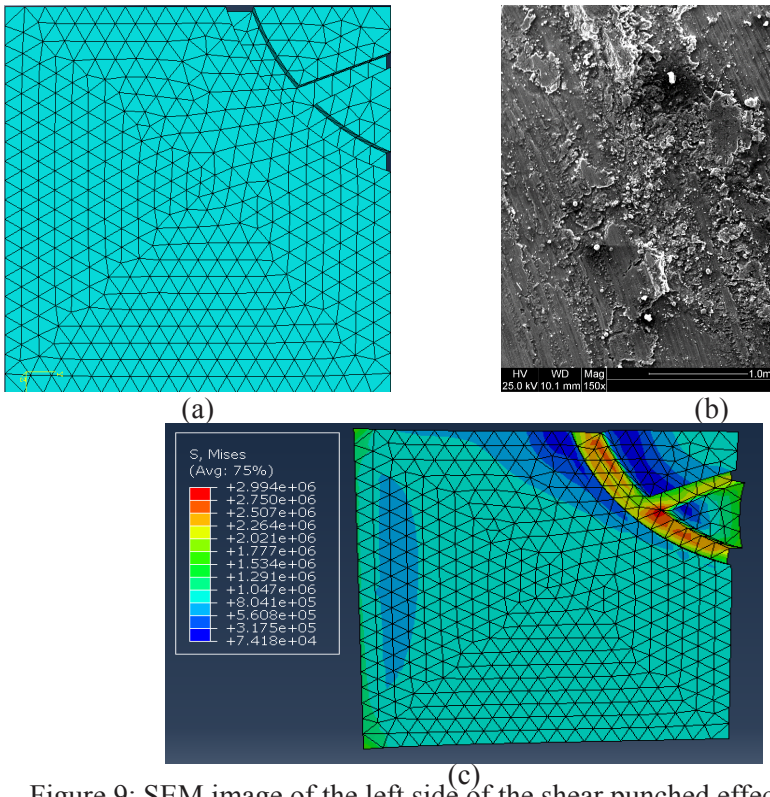

Figure 9: SEM image of the left side of the shear punched effect for AZ81 specimen. (a) Finite element meshes (b) SEM photo (c) finite element result

Regarding Fig. 9, likely, there is some dust and there are some ups and downs on the surface of the specimen. It was maybe due to the specimen damage before the test or casting defect on the Mg FSPed sheet. As it can be seen from fig. 9 that the exerted force leads the stress to increase rather than the region far from the cracks. It is also worth mentioning that maximum amount is 100 times greater than the minimum counterpart due to the fact that

5 CONCLUSION

In this paper, the investigation on the crack and defect detection of the metals for the pipelines has been done. The experimental setup consists of a circulation water system for the pipelines and the finite element simulation has been done on the metal samples. The achieved results based on the simulation and SEM are as bellow:

- Finite Element simulation for post processing indicate that the maximum load at the final step size in the simulation plays an important role in distribution of maximum

stress around the cracks.

- As it was clear from Fig. 9, the amount of maximum stress distribution varies through the circular crack and the amount of this maximum is approximately 3 MPa.
- Crack initiation and growth will occur in the regions with highest intensity factor.
- Numerical simulation indicates that in the region with minimum stress field, the crack initiation will not occur and the experiment validate this phenomenon in Fig. 9.

REFERENCES

A. NourollahiI, G., Farahani, M. A., Babakhaniii & Mirjavadi, S. S. (2013). Compressive Deformation Behavior Modeling of AZ31 Magnesium Alloy at Elevated Temperature Considering the Strain Effect.

Ayadi, A., Ghorbel, O., BenSalah, M. S. & Abid, M. (2019). Kernelized technique for outliers detection to monitoring water pipeline based on WSNs. *Computer Networks,* 150: 179-189.

Bahadori, A. (2017). Chapter 1 - Transportation Pipelines. Oil and Gas Pipelines and Piping Systems. A. Bahadori. Boston, *Gulf Professional Publishing***:** 1-27.

Chang, Y., Zi, Y., Zhao, J., Yang, Z., He, W. & Sun, H. (2017). An adaptive sparse deconvolution method for distinguishing the overlapping echoes of ultrasonic guided waves for pipeline crack inspection. *Measurement Science and Technology*, *28*(3): 035002.

Chen, X., Zhou, F., Chen, X. & Yang, J. (2019). Mobile visual detecting system with a catadioptric vision sensor in pipeline. *Optik*, 193: 162854.

Forsat, M. (2019). Investigating nonlinear vibrations of higher-order hyper-elastic beams using the Hamiltonian method. *Acta Mechanica.*

Hawari, A., Alamin, M., Alkadour, F., Elmasry, M. & Zayed, T. (2018). Automated defect detection tool for closed circuit television (cctv) inspected sewer pipelines. *Automation in Construction,* 89: 99-109.

Jin, H., Zhang, L., Liang, W. & Ding, Q. (2014). Integrated leakage detection and localization model for gas pipelines based on the acoustic wave method. *Journal of Loss Prevention in the Process Industries*, 27: 74-88.

Liu, C., Li, Y., Fang, L. & Xu, M. (2017). Experimental study on a de-noising system for gas and oil pipelines based on an acoustic leak detection and location method. *International Journal of Pressure Vessels and Piping*, 151: 20-34.

Lowe, M. J. S., Alleyne, D. N. & Cawley, P. (1998). Defect detection in pipes using guided waves. *Ultrasonics*, *36*(1): 147-154.

Mao, D., Chu, G., Yang, L. & Li, Z. (2015). Deepwater Pipeline Damage and Research on Countermeasure. *Aquatic Procedia*, 3: 180-190.

Mirjavadi, S. S., Forsat, M., Barati, M., Abdella, G., Mohasel afshari, B., Hamouda, A. M. S. & Rabby, S. (2019). Dynamic response of metal foam FG porous cylindrical micro-shells due to moving loads with strain gradient size-dependency.

Mirjavadi, S. S., Forsat, M., Hamouda, A. M. S. & Barati, M. R. (2019). Dynamic response of functionally graded graphene nanoplatelet reinforced shells with porosity distributions under transverse dynamic loads. *Materials Research Express*, *6*(7): 075045.

Mirjavadi, S. S., Forsat, M., Nikookar, M., Barati, M. R. & Hamouda, A. M. S. (2019). Nonlinear

forced vibrations of sandwich smart nanobeams with two-phase piezo-magnetic face sheets. *The European Physical Journal Plus*, *134*(10): 508.

Singh, R. (2017). *5 - Hazards and Threats to a Pipeline System. Pipeline Integrity Handbook* (Second Edition). R. Singh, Gulf Professional Publishing, 35-88.

Sousa, E. O., Cruz, S. L. & Pereira, J. A. F. R. (2009). Monitoring pipelines through acoustic method. Computer aided chemical engineering. De Brito Alves, R. M., do Nascimento, C. A. O. & Biscaia, E. C. *Elsevier*, 27: 1509-1514.

Stewart, M. (2016). *14 - Pipeline operations. Surface Production Operations*. M. Stewart. Boston, Gulf Professional Publishing**:** 961-979.

Xu, Q., Zhang, L. & Liang, W. (2013). Acoustic detection technology for gas pipeline leakage. *Process Safety and Environmental Protection*, *91*(4): 253-261.

Zajam, S., Joshi, T. & Bhattacharya, B. (2019). Application of wavelet analysis and machine learning on vibration data from gas pipelines for structural health monitoring. *Procedia Structural Integrity*, 14: 712-719.

Zeng, X., Dong, F.-F., Xie, X.-D. & Du, G.-F. (2019). A new analytical method of strain and deformation of pipeline under fault movement. *International Journal of Pressure Vessels and Piping*, 172: 199-211.

Cite this article as: Forsat M., Hamouda A. S., "The Investigation of an Efficient and Effective Proactive Pipeline Integrity System", *International Conference on Civil Infrastructure and Construction (CIC 2020)*, Doha, Qatar, 2-5 February 2020, DOI: https://doi.org/10.29117/cic.2020.0124